**Daniela Cecconi**[1]
**Stefano Orzetti**[1]
**Elodie Vandelle**[1]
**Sara Rinalducci**[2]
**Lello Zolla**[2]
**Massimo Delledonne**[1]

[1]Dipartimento di Biotecnologie, University of Verona, Verona, Italy
[2]Dipartimento di Scienze Ambientali, University of Tuscia, Viterbo, Italy

Received December 19, 2008
Revised February 17, 2009
Accepted February 23, 2009

Research Article

# Protein nitration during defense response in *Arabidopsis thaliana*

Nitric oxide and reactive oxygen species play a key role in the plant hypersensitive disease resistance response, and protein tyrosine nitration is emerging as an important mechanism of their co-operative interaction. Up to now, the proteins targeted by this post-translational modification in plants are still totally unknown. In this study, we analyzed for the first time proteins undergoing nitration during the hypersensitive response by analyzing *via* 1D- and 2D-western blot the protein extracts from *Arabidopsis thaliana* plants challenged with an avirulent bacterial pathogen (*Pseudomonas syringae pv. Tomato*). We show that the plant disease resistance response is correlated with a modulation of nitration of proteins involved in important cellular process, such as photosynthesis, glycolysis and nitrate assimilation. These findings shed new light on the signaling functions of nitric oxide and reactive oxygen species, paving the way on studies on the role of this post-translational modification in plants.

**Keywords:**
*Arabidopsis thaliana* / Hypersensitive response / Protein nitration / Proteomics
DOI 10.1002/elps.200800826

## 1 Introduction

Nitric oxide (NO) is an important endogenous signaling molecule that mediates many plant developmental and physiological processes during the entire life of the plant, from germination to fruit maturation and senescence [1], and that functions in the plant responses to abiotic and biotic stresses [2–4]. In particular, under pathogen attack it plays a central role during the onset of the hypersensitive reaction (HR), a defence response characterized by the formation of necrotic lesions at the infection site that restricts pathogen infection and spread [5]. The HR shows some regulatory and mechanistic features characteristic of apoptosis in animal cells [6] and is associated with the systemic acquired resistance, a mechanism of induced defence that confers long-lasting protection against a broad spectrum of microorganisms [7].

**Correspondence:** Professor Massimo Delledonne, Dipartimento di Biotecnologie, Università degli Studi di Verona, Strada le Grazie 15, 37134 Verona, Italy
**E-mail:** massimo.delledonne@univr.it
**Fax:** +39-045-8027962

**Abbreviations: 2D-WB,** two-dimensional Western blot**; GO,** gene ontology**; hpi,** hours post infection**; HR,** hypersensitive response**; NO,** nitric oxide**; NT,** not treated**; Pst,** *Pseudomonas syringae pv. tomato***; ROS,** reactive oxygen species**; RT,** room temperature**; SSP,** standard spot number

One of the earliest events in the HR is the rapid accumulation of reactive oxygen species (ROS) [8] and NO [9], which cooperate in a fine-tuned balance to trigger the hypersensitive cell death [10]. Both NO and ROS are also components of a highly integrated defence system that triggers the local expression of resistance genes, although NO functions independently of ROS in the induction of various defence genes including pathogenesis-related proteins and enzymes of phenylpropanoid metabolism involved in the production of lignin, antimicrobials and the secondary signal salicylic acid [11].

NO signaling functions depend on its reactivity, and ROS are key modulators of NO in triggering cell death, although through mechanisms different from those commonly observed in animals [10]. In many biological systems, the cytotoxic effects of NO and ROS derive from the diffusion-limited reaction of NO with $O_2^-$ to form the peroxynitrite anion $ONOO^-$, which then interacts with several cellular components and leads to cellular damages [12]. Despite substantial experimental evidence suggesting that secondary oxidants derived from NO are responsible for cytoxicity and associated tissue injury [13], in plants $ONOO^-$ is not an essential mediator of NO/ROS induced cell death [10, 14]. $ONOO^-$ is a powerful oxidant, causing lipid peroxidation, oxidation of protein associated thiol groups and nitration of protein tyrosine residues [15]. Tyrosine-nitration, a process by which a nitrite group is added to the ortho-position of Tyr residues forming 3-nitrotyrosine, may alter protein conformation and structure, catalytic activity

and/or susceptibility to protease digestion. Nitration of Tyr residues may also interfere with signaling processes associated with protein Tyr phosphorylation. For example, it has been shown that nitration of a single Tyr residue in purified CDC2, a cell cycle kinase, prevents its phosphorylation on Tyr [16]. Therefore, Tyr-phosphorylation is a good candidate for mediating signaling events induced by $ONOO^-$ [17] and depending on $ONOO^-$ local concentrations, nitration and phosphorylation of critical Tyr residues may be competing processes [18].

Up to now, evidence for Tyr-nitration in plants has been reported in nitrite reductase antisense tobacco plants displaying a high NO emission rate [19], in tobacco cells treated with the elicitor INF1 [20], in olive leaves exposed to abiotic stress [21, 22] and in *Arabidopsis thaliana* plants challenged with an incompatible bacterial pathogen [23]. However, the proteins targeted by this post-translational modification are still totally unknown.

The application of proteomics in plant pathology is becoming more commonplace with techniques such 2-DE and MS being used to identify changes in protein levels in plant upon infection by pathogenic organisms [24]. We already described the application of proteomic tools for the detection of S-nitrosylated proteins during the time course of the HR in *A. thaliana* challenged with an avirulent bacterial pathogen [25]. In this study, we used these proteomic tools to deepen the understanding about the regulatory function of NO species, in particular $ONOO^-$, to identify Tyr-nitrated proteins in *A. thaliana* undergoing HR.

## 2 Materials and methods

### 2.1 Chemicals

Peroxynitrite was purchased from Calbiochem (San Diego, CA, USA).

### 2.2 Growth of *A. thaliana*

*A. thaliana* L. (Columbia ecotype Col0) seeds were sown on sterile soil, vernalized for 1 day at 4°C and grown at 24°C and 60% relative humidity, with 8 h light at 120 μmol quanta $m^2$/s, and 16 h dark.

### 2.3 Bacterial culture and inoculation

The avirulent *Pseudomonas syringae* pv. *tomato* (Pst) DC3000 strain carrying *AvrB* gene was grown in King's B medium (MKB; 2% w/v Proteose Peptone, 6.1 mM $MgSO_4$, 8.6 mM $K_2HPO_4$, and 1% v/v glycerol [pH 7.2], added with 50 mg/mL kanamycin and 50 mg/mL rifampin) at 28°C overnight. Bacterial suspension was infiltrated at a final concentration of $1 \times 10^8$ cfu/mL in 10 mM $MgCl_2$ into the abaxial surface of ten *A. thaliana* leaves using a hypodermic syringe without needle. As controls, leaves were infiltrated with 10 mM $MgCl_2$ or not treated (NT). *A. thaliana* leaves were then collected from plants 4, 8, 12, 16, and 24 h after infiltration and kept frozen (−80°C) until protein extraction.

### 2.4 Peroxynitrite treatment

ONOOH is a short-lived molecule and spontaneously decays to nitrate [26]. Stock concentration was determined spectrophotometrically at 302 nm using $\varepsilon_{302}$ 1670 $M^{-1}$/cm. Plant treatment with $ONOO^-$ was performed as previously described [23] with minor modifications. Solution of "fresh" $ONOO^-$ (3 mM) was prepared by dilution into water immediately before use. Peroxynitrite solution was infiltrated into the abaxial surface of *A. thaliana* leaves using a hypodermic syringe without a needle. *A. thaliana* leaves ($OONO^-$ infiltrated) were harvested from plants 5 min after infiltration and kept frozen (−80°C) until protein extraction.

### 2.5 Protein extraction and solubilization

For protein extraction, ten frozen leaves (pooled from five different plants NT and after Pst or $ONOO^-$ inoculation) were ground to a fine powder (about 400 mg) in a mortar placed in a liquid nitrogen bath, in the presence of a frozen droplet of a protease inhibitor mixture (1 × Complete tablet, Roche Molecular Biochemicals, Mannheim, Germany). Protein extraction was performed in 3 mL of a 2-D solubilizing/lysing solution: 7 M urea (Sigma–Aldrich), 2 M thiourea (Sigma), 3% w/v CHAPS (Sigma), 2% w/v amido-sulpho betaine 14 (ASB14), 20 mM Tris (Sigma) and 1 × Complete, Mini protease inhibitor cocktail tablet (Roche). The samples were sonicated 5 × 30 s on ice with 1 min break between the sonications, and 1% v/v pH 3–10 Ampholyte (Fluka, Buchs SG Switzerland) was added. After 1 h with gentle agitation the samples were centrifuged for 30 min at 14 000 × *g* at 4°C to remove the nucleic acids (complexed with ampholytes), as well as cellular debris, and unsolubilized compounds. To completely remove all the interfering compounds/molecules (including chlorophyll), proteins were precipitated in an acetone:methanol solution (8:1 v/v). Samples were left at 20°C overnight and then centrifuged at 14 000 × *g* for 10 min. The supernatants were discarded and the pellets obtained were re-solubilized in 2-D solubilizing/lysing solution. The supernatants were incubated in a solution of 5 mM tributyl phosphine and 10 mM acrylamide for 60 min at room temperature (RT) to reduce protein disulphide bonds and alkylate the cysteine thiolic groups. The reaction was blocked by the addition of 10 mM DTT (Sigma), and samples were collected and stored at −80°C. The protein concentration was evaluated with DC Protein assay (Bio-Rad) based on the Lowry method. The calibration curve was obtained by using known concentrations of BSA dissolved in distilled water.

 

### 2.6 1-DE

1-D SDS-PAGE was performed according to Laemmli [27] using 12% acrylamide gels. Briefly, protein extracts (from NT or Pst infiltrated leaves) were diluted 1:1 with Laemmli's sample buffer (62.5 mM Tris-HCl, pH 6.8, 25% v/v glycerol, 2% w/v SDS, 0.01% w/v bromophenol blue and 5% β-mercaptoethanol), and boiled for 3 min. The applied amount of protein sample per lane was 30 μg; moreover, the Precision Plus Protein Standards (Bio-Rad) was used as a standard for molecular weight determination. The electrophoresis was conducted in a Mini PROTEAN 3 Cell (Bio-Rad) with Tris/glycine/SDS running buffer (192 mM glycine, 0.1% w/v SDS and Tris to pH 8.3) by setting 130 V until the tracking dye, bromophenol blue, reached the anodic end of the gels. The experiment was repeated three times.

### 2.7 2-DE

Seven centimeter long, pH 4–7 immobilized pH gradient strips (IPG; Bio-Rad) were rehydrated for 4 h with 150 μL of 2-D solubilizing solution (7 M urea, 2 M thiourea, 3% w/v CHAPS and 20 mM Tris) containing 1 mg/mL of total protein extract (from NT, $ONOO^-$ or Pst infiltrated leaves). IEF was carried out with a Protean IEF Cell (Bio-Rad), with a low initial voltage and then by applying a voltage gradient up to 5000 V with a limiting current of 50 μA/strip. The total product time × voltage applied was 25 000 Vh for each strip and the temperature was set at 20°C. For the second dimension, the IPG strips were equilibrated for 26 min by rocking in a solution of 6 M urea, 2% w/v SDS, 20% v/v glycerol and 375 mM Tris-HCl, pH 8.8. The IPG strips were then laid on an 8–18% gradient SDS-PAGE with 0.8% w/v agarose in Tris/glycine/SDS running buffer. The second dimension was performed in a Mini PROTEAN 3 Cell (Bio-Rad) with Tris/glycine/SDS running buffer. The electrophoresis was conducted by setting a current of 5 mA for each gel for 1 h, then 10 mA/gel for 1 h and 20 mA/gel until the tracking dye, bromophenol blue, reached the anodic end of the gels. The experiment was repeated four times for each sample (NT, $ONOO^-$ or Pst infiltrated leaves).

### 2.8 Western blot analysis

Proteins (extracted from NT and Pst or $ONOO^-$ infiltrated leaves and separated by 1D or 2D gels) were electrophoretically transferred to PVDF membranes (GE Healthcare) using a Mini Trans Blot Cell (Bio-Rad) at 60 V for 2 h. Moreover, for nitroprotein identification proteins in 2D gels were partially transferred to PVDF membranes at 320 mA/gel for 10 min. Proteins remaining in the gels were then visualized by Sypro Ruby and excised for MS analysis.

Membranes were stained with Ponceau S (Sigma–Aldrich) to confirm equal protein loading and then blocked by incubating with 1% w/v bovine serum albumin in 0.2% v/v Tween-20 Tris-buffered saline (20 mM Tris, 150 mM NaCl, pH 7.6) for 1 h at RT. The membranes were then incubated with a monoclonal antibody against 3-nitrotyrosine (1:2000 dilution; 1A6 clone, Upstate Biotechnology, Lake Placid, NY, USA) for 3 h at RT in blocking solution. The membranes were then washed four times in 0.2% v/v Tween-20 Tris-buffered saline and probed with ECL anti-mouse IgG HRP-linked (Amersham Biosciences, Uppsala, Sweden) at 1:10 000 dilution for 1 h at RT in blocking solution. The immunocomplexes were detected by chemiluminescence (ECL, Amersham Biosciences) on X-Omat AR (Kodak, Rochester, NY, USA) film.

To eliminate any possible false-positive results associated with nonspecific binding of the anti-3-nitrotyrosine antibody, control experiments were performed in which the PVDF membrane was reduced with sodium dithionite before Western blot analysis. Briefly, reduction of nitrotyrosine to aminotyrosine was achieved by treating one membrane with 10 mM sodium dithionite in 50 mM pyridine-acetate buffer, pH 5.0, for 1 h at RT. After the reaction, the membrane was rinsed with distilled water and then equilibrated with 0.2 % v/v Tween-20 Tris-buffered saline. The experiment was repeated three times for 1D- and two-dimensional Western blot (2D-WB) analysis of $ONOO^-$ infiltrated leaves and four times for 2D-WB analysis of protein sample extracted from NT or Pst infiltrated leaves.

### 2.9 Image analysis

Gels and X-ray film replicas were scanned with a VersaDoc 1000 imaging system (Bio-Rad), and the intensity of chemiluminescence and of Sypro Ruby staining was measured using Quantity One software v. 4.4 (Bio-Rad) or PDQuest 2D software v. 7.3 (Bio-Rad) for one- or two-dimensional analyses respectively. Concerning the 2D-WB image analysis, each X-ray film image was analyzed for spot detection, background subtraction and protein spot OD intensity quantification. The image showing the higher number of spots and the best protein pattern was chosen as a reference template, and spots in a standard image were then matched across the four replicated films. Seven different standard images were obtained (representative of NT, $ONOO^-$ and 4, 8, 12, 16, 24 h Pst-infiltrated plants), including the spots present at least in two among the four replicas produced. The comparisons were performed among standard images representative of NT, $ONOO^-$ and 4, 8, 12, 16, 24 h Pst-infiltrated plants. Data were log transformed and analysed with Student's *t*-test, spots giving significant results ($p < 0.05$) were verified visually to exclude artefacts.

### 2.10 In-gel digestion and nitroprotein identification by nano RP-HPLC-ESI-MS/MS

Spots showing an immunostaining after the $ONOO^-$ infiltration were carefully cut out from 2-D Sypro Ruby stained gels and subjected to in-gel trypsin digestion as

 

previously described [28]. Briefly, the digestion was performed using 12.5 ng/μL of trypsin (modified porcine trypsin, sequencing grade, Promega, Madison, WI, USA) at 37°C overnight. The supernatant containing the extracted tryptic peptides was dried by vacuum centrifugation and the peptide mixtures were redissolved in 10 μL of 5% v/v formic acid. Peptide mixtures were separated using a nanoflow-HPLC system (Ultimate; Switchos; Famos; LC Packings, Amsterdam, The Netherlands). A sample volume of 10 μL was loaded by the autosampler onto a homemade 2 cm fused silica precolumn (75 μm I.D.; 375 μm O.D.; Reprosil C18-AQ, 3 μm (Ammerbuch-Entringen, Germany)) at a flow rate of 2 μL/min. Sequential elution of peptides was accomplished using a flow rate of 200 nL/min and a linear gradient from Solution A (2% acetonitrile; 0.1% formic acid) to 50% v/v of Solution B (98% v/v acetonitrile; 0.1% v/v formic acid) in 40 min over the precolumn in-line with a homemade 10–15 cm resolving column (75 μm I.D.; 375 μm O.D.; Reprosil C18-AQ, 3 μm (Ammerbuch-Entringen)). Peptides were eluted directly into a high capacity ion trap (model HCTplus Bruker-Daltonik, Germany). Capillary voltage was 1.5–2 kV and a dry gas flow rate of 10 L/min was used with a temperature of 200°C. The scan range used was from 300 to 1800 $m/z$. Protein identification was performed by searching in the National Center for Biotechnology Information nonredundant database (NCBInr) using the MASCOT program (Matrix Sciences, London, UK). The following parameters were adopted for database searches: tyrosine nitration, complete propionamide of cysteines and partial oxidation of methionines, N-acetylation, peptide mass tolerance ± 1.2 Da, Fragment mass tolerance ± 0.9 Da and missed cleavages of 2. For positive identification, the score of the result of $[-10 \times \mathrm{Log}(P)]$ had to be over the significance threshold level ($p < 0.05$).

### 2.11 Protein categorization

Gene ontology (GO) lists were downloaded using the tool FatiGO [29] from Babelomics (http://fatigo.bioinfo.cipf.es/), which includes a complete suite of web tools for the functional analysis of groups of genes in high-throughput experiments along with the use of information on GO terms. Each protein was classified with respect to its cellular component, biological process and molecular function using GO annotation. When no GO annotation was available, proteins were annotated manually based on literature searches and closely related homologues.

## 3 Results

### 3.1 Identification of nitrated proteins in *A. thaliana* by 2D-WB and MS

To identify Tyr-nitrated proteins in *A. thaliana*, we used an approach based on 2D electrophoresis combined with Western blot using an anti-nitroTyr antibody. We first tested the reliability of this approach by analyzing Tyr-nitrated proteins in plant leaves infiltrated with commercial $ONOO^-$. Proteins were extracted from leaves exposed for 5 min to 3 mM peroxynitrite, using optimized conditions to prevent proteolytic breakdown and to limit artificial modifications. Then, protein extracts were fractionated by 2-DE, partially transferred to PVDF membrane, and analyzed by 2D-WB analysis with an anti-nitroTyr antibody. Using this method a total of 19 nitroTyr-immunoreactive spots were detected (Fig. 1A). As a control, we treated PVDF membrane with dithionite prior to incubation with the anti-nitroTyr antibody. This treatment converts nitroTyr in aminoTyr, allowing the detection of false positive spots. After dithionite treatment, only one spot was detected, which could correspond to unspecific immunoreactivity of the antibody (Fig. 1B). Three technical replicates were carried out for the $ONOO^-$ and the dithionite-treated samples. The 18 positive Tyr-nitrated proteins were then excised from the parent Sypro Ruby-stained gels (Fig. 1C), digested with trypsin and subjected to RP-HPLC-ESI-MS/MS analysis for protein identification. Out of 18 immunoreactive spots, 12 have been successfully identified as members of different protein families. These proteins are presented in Table 1 with the standard spot number (SSP), the identification parameters (Supporting Information Table 1 with peptide sequences is provided in Supporting Information) and the indication of their GO annotation (cellular component, biological process and molecular function) and in Fig. 2 marked with the SSP.

As observed in Table 1, these 12 spots correspond to only eight different proteins undergoing Tyr-nitration *in vivo* in *A. thaliana*, namely 33-kDa oxygen-evolving protein of photosystem II (PsbO1 and PsbO2), ATP synthase CF1 α subunit (CF1-ATPase α), RuBisCO large subunit, RuBisCO activase, Fructose-bisphosphate aldolase 1 (FBA1), Fructose-bisphosphate aldolase 2 (FBA2) and Glutamine synthetase 2 (GS2). This result suggests that six out of the 12 identified immunoreactive spots correspond to different isoforms of the same Tyr-nitrated protein or that one protein could be Tyr-nitrated one or several times. Unfortunately, all nitro-Tyr-containing peptides were below detection limits of the instrument, likely due to the high liability of this modification. Until recently, the lack of specific enrichment and sensitive identification methods for nitrated residues has prevented the analysis of such low-level protein modifications, especially *in vivo*. For this reason, we have not been able to determine the site(s) of Tyr-nitration.

### 3.2 Western blot analysis of Tyr-nitrated proteins during the HR in *A. thaliana*

To monitor changes in the nitroproteome during the progression of the hypersensitive disease resistance response, *A. thaliana* plants were challenged with the incompatible bacterial pathogen Pst carrying the *avrB*

 

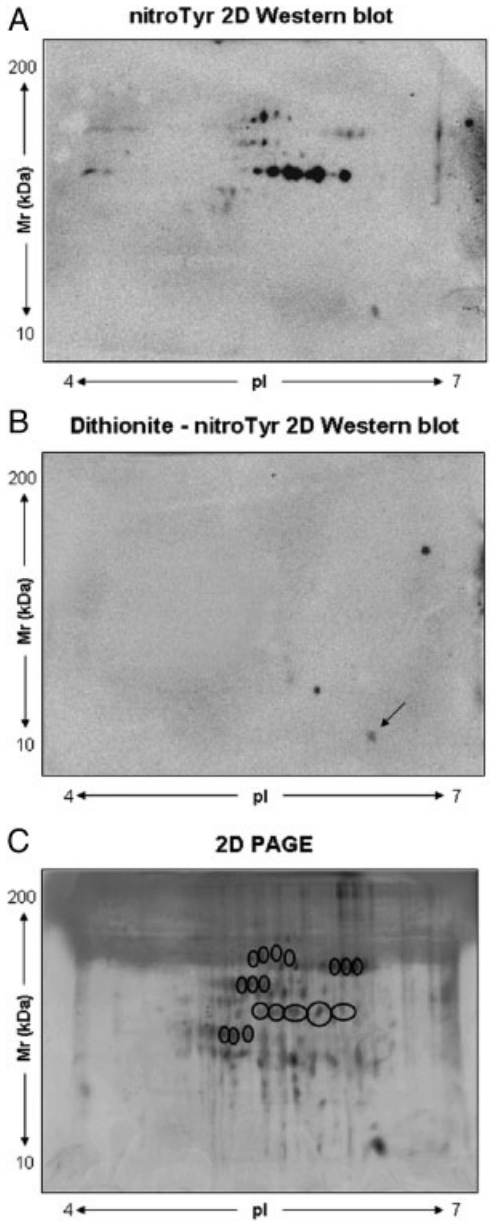


**Figure 1.** Analysis of nitroproteome of *A. thaliana* using a proteome-based strategy. Representative 2D-WB (A) before and (B) after reduction of nitrotyrosine to aminotyrosine are shown. (C) Parent Sypro Ruby-stained gel, together with matching immunoreactive spots (marked by ellipses), is also shown.

avirulence gene. Leaves were harvested at different time points after infection and protein extracts were separated by 1-DE and subjected to WB analysis with the anti-nitroTyr antibody. As controls, proteins were also extracted from NT and $MgCl_2$ infiltrated leaves; since no differences have been observed between both controls (data not shown), only NT samples are presented. Western blot analysis revealed that Tyr-nitrated proteins are present in NT samples and during the entire time course of infection (Fig. 3) and, although the pattern does not show any significant difference, a strong increase in the signal at 4 and 8 hours post infection (hpi) can be observed. Because of the weak resolution of one-dimensional protein separation, we further adopted 2D-WB to analyze Tyr-nitrated during the HR process. Four reproducible 2D-WB replicates were obtained for each time point (4, 8, 12, 16 and 24 hpi and NT; Supporting Information Fig. 1). By image analysis using PDQuest program, the number of immunoreactive spots corresponding to potential Tyr-nitrated proteins were evaluated for each sample: 29 spots were detected in the NT control 2D-WB standard image, *versus* 36, 35, 26, 28 and 26 spots in the 2D-WB standard images corresponding to 4, 8, 12, 16 and 24 hpi, respectively (Fig. 4). 2D-WB standard image overlay revealed a total of 16 spots showing signal intensity variation between the different time points after pathogen infection (the semi-quantitative data obtained by 2D-WB regarding normalized volume and fold changes of regulated spots are reported in Supporting Information Table 2). Out of these 16 spots, 12 were identified and correspond to proteins differentially Tyr-nitrated during HR corresponded to nitroproteins previously identified after commercial $ONOO^-$-infiltration (see Fig. 2): FBA1, FBA2 and RuBisCO large subunit showed the strongest Tyr-nitration level at 4 hpi, whereas RuBisCO activase, CF1-ATPase α and GS2 at 8 hpi, PsbO1 and PsbO2 at 16 hpi. Only four spots presenting a modulation in Tyr-nitration level were not successfully identified because of their relative low amount in the partially transferred gels.

## 4 Discussion

In this study we identified for the first time proteins undergoing nitration during the HR by analyzing *via* 1D- and 2D-WB the protein extracts from *A. thaliana* plants challenged with an avirulent bacterial pathogen. By one dimensional Western blot analysis we found that Tyr nitration level was particularly enhanced after 4 and 8 h exposure hpi, confirming that Tyr-nitration could be a relevant physiological process during the HR in plants, as previously demonstrated [23]. We therefore investigated, for the first time in plants, the nitroproteome by 2D-WB approach. The patterns we obtained from 2D-WB analysis were highly reproducible and, by the comparison of the standard images, a modulation in relative immunostaining signal for some spots was detected. The corresponding spots were excised from ONOO-infiltrated plant parent gel and subjected to MS analysis. Interestingly, none of the identified proteins have been previously reported to be nitrated in plant. However, these proteins should be considered putatively nitrated until the nitrated sites have been identified by sequence analysis. The identified nitrated proteins (that were also found to be regulated during the HR) fell into different functional categories (Table 1). Among the nitrated proteins involved in light phase of photosynthesis were two isoforms of 33-kDa oxygen-evolving protein of photosystem II (PsbO1 and PsbO2). PsbO protein is conserved in all known oxygenic photo-

 

**Table 1.** Identified nitrated proteins of *A. thaliana*

| Spot no. | Protein name | Locus ID | NCBI accession number | p*I*/$M_r$ Theor | p*I*/$M_r$ Exper | Sequence coverage (%) | Number matched peptides | MASCOT Score | GO biological process | GO cellular component | GO molecular function |
|---|---|---|---|---|---|---|---|---|---|---|---|
| *Photosynthesis (light phase)* | | | | | | | | | | | |
| 1 | PsbO2 (33-kDa oxygen-evolving protein of photosystem II) | At3g50820 | gi\|15230324 | 5,92/35,2 | 5,9/32 | 53 | 16 | 798 | Photosystem II assembly | Chloroplast | Oxygen evolving activity |
| 2 | PsbO2 (33-kDa oxygen-evolving protein of photosystem II) | At3g50820 | gi\|15230324 | 5,92/35,2 | 5,7/32 | 58 | 16 | 837 | Photosystem II assembly | Chloroplast | Oxygen evolving activity |
| 3 | PsbO1 (33-kDa oxygen-evolving protein of photosystem II) | At5g66570 | gi\|22571 | 5,68/35,2 | 5,5/32 | 17 | 6 | 304 | Photosystem II assembly | Chloroplast | Oxygen evolving activity |
| *ATP synthesis* | | | | | | | | | | | |
| 4 | ATP synthase CF1 $\alpha$ subunit | AtCg00120 | gi\|7525018 | 5,19/55,3 | 5,5/55 | 27 | 12 | 640 | dATP biosynthetic process | Chloroplast | ATPase activity |
| *Calvin cycle and glycolysis* | | | | | | | | | | | |
| 5 | RuBisCO large subunit | AtCg00490 | gi\|7525041 | 5,88/53,4 | 6/54,5 | 45 | 24 | 1208 | C utilization by fixation of CO2 | Chloroplast | Ribulose-bisphosphate carboxylase activity |
| 6 | RuBisCO large subunit | AtCg00490 | gi\|7525041 | 5,88/53,4 | 6,2/54,5 | 42 | 21 | 1028 | C utilization by fixation of CO2 | Chloroplast | Ribulose-bisphosphate carboxylase activity |
| 7 | RuBisCO large subunit | AtCg00490 | gi\|7525041 | 5,88/53,4 | 6,4/54,5 | 36 | 18 | 870 | C utilization by fixation of CO2 | Chloroplast | Ribulose-bisphosphate carboxylase activity |
| 8 | RuBisCO activase | At2g39730 | gi\|18405145 | 5,87/52,3 | 5,5/55 | 36 | 13 | 730 | Response to cold and light stimulus | Chloroplast | Enzyme regulator activity |
| 9 | Fructose-bisphosphate aldolase 1 | At2g21330 | gi\|18399660 | 6,18/43 | 5,5/43 | 27 | 11 | 529 | Pentose phosphate shunt | Chloroplast | Aldolase activity |
| 10 | Fructose-bisphosphate aldolase 1 | At2g21330 | gi\|18399660 | 6,18/43 | 5,7/43 | 45 | 17 | 854 | Pentose phosphate shunt | Chloroplast | Aldolase activity |
| 11 | Fructose-bisphosphate aldolase 2 | At4g38970 | gi\|18420348 | 6,78/43,1 | 5,9/43 | 35 | 13 | 656 | Pentose phosphate shunt | Cytosol | Aldolase activity |
| *Nitrate assimilation* | | | | | | | | | | | |
| 12 | Glutamine synthetase 2 | At5g35630 | gi\|15238559 | 6,43/47,7 | 5,5/55 | 27 | 14 | 768 | Ammonia assimilation cycle | Chloroplast, mitochondrion | Glutamate-ammonia ligase activity |

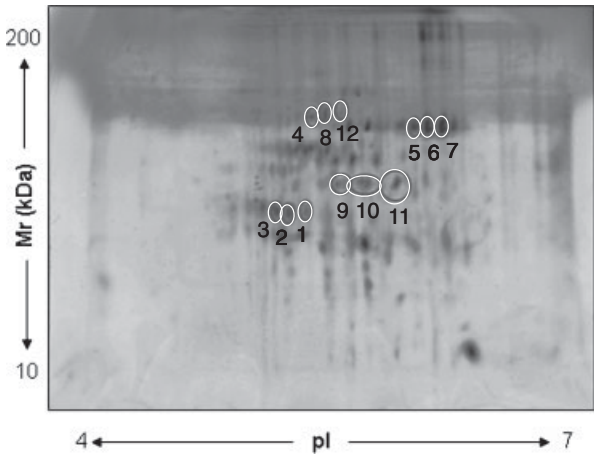


**Figure 2.** Identified nitrated proteins of *A. thaliana*. Representative two-dimensional map of ONOO-infiltrated leaves, showing identified nitrated proteins. The corresponding spots are marked with the SSP reported in the Table 1.

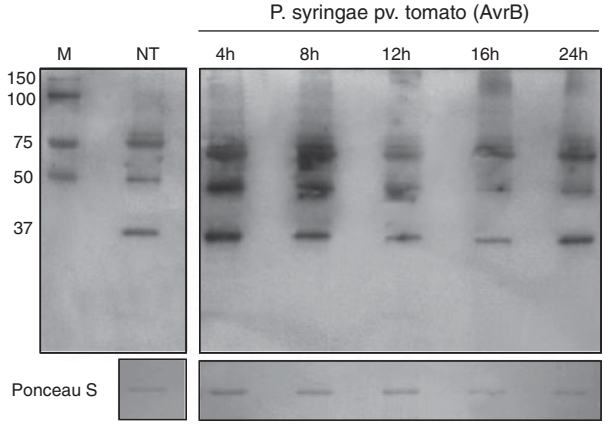


**Figure 3.** 1D Western blot analysis of nitrated proteins during the HR in *A. thaliana*. A total protein extract from *A. thaliana* control (NT), and 4, 8, 12, 16, and 24 h after infiltration with avirulent Pst (lanes 2–7, 30 μg/lane) were electrophoresed on 12% SDS polyacrylamide gels, blotted to PVDF membrane, and probed with a monoclonal anti-nitrotyrosine antibody. A Ponceau S stain of the ribulose bisphosphate carboxylase-oxygenase is shown at the bottom for control of protein loading.

synthetic organisms, and is located on the lumenal side of PSII. It is responsible for water oxidation, and produces molecular oxygen as a by-product [30]. In addition to this role, several auxiliary roles have been proposed for PsbO, including calcium binding, manganese stabilizing/binding, carbonic anhydrase, stability of the PSII dimeric structure and GTP binding [31]. Interestingly, PsbO is represented by two isoforms in *A. thaliana*, namely PsbO1 and PsbO2 [32, 33]. Notably, PsbO2 has a three-fold higher GTPase activity than PsbO1, and so it represents the main GTPase in *A. thaliana* PSII. In particular, it has been demonstrated that PsbO2 GTPase activity is involved in dephosphorylation and degradation of PSII reaction centre D1 protein [34]. It has also been reported that PsbO2 is upregulated [35], and modified by malondialdehyde [36] during oxidative stress in *A. thaliana*. Interestingly, a correlation between oxidative stress and the HR has been already demonstrated [37, 10]. Accordingly, the PsbO2 levels were found to be upregulated in *A. thaliana* after inoculation with the avirulent (avrRpm1) strain of *P. syringae* [38]. It has also been demonstrated that Tyr residues of the PsbO are poorly concealed in the protein matrix and so visibly exposed to the medium [39]. Moreover, it has been suggested that nitration of the Tyr-containing PSII polypeptides could be enhanced by the presence of $Fe^{2+}$ and Mn ions [40]. In agreement with these observations, we were able to show that two nitrated PsbO2 isoforms and one PsbO1 isoform are induced after exposure of *A. thaliana* with the avirulent (avrB) strain of *P. syringae*. Our results suggest that during HR, PsbO2 protein undergo nitration at more than one TYR residue, resulting in different p*I*s.

Another nitrated protein whose nitration was upregulated during HR was chloroplastic ATP synthase CF1 α subunit (CF1-ATPase α). This protein sticks into chloroplast stroma, where dark reactions of photosynthesis and ATP synthesis take place. By a proteomic analysis of *A. thaliana* it has been reported that CF1-ATPase α subunit is the target of NO-induced S-nitrosylation [41]. Moreover, CF1-ATPase α subunit levels were found to be upregulated in *A. thaliana* during the HR elicited by the avirulent (avrRpm1) strain of *P. syringae* [38]. Here, we reported that nitrated CF1-ATPase α is induced in *A. thaliana* challenged with the avirulent (avrB) strain of *P. syringae*. Our data confirm the involvement of CF1-ATPase α during HR, and suggest that TYR nitration of this protein may play an important role in plant defence.

Among the nitrated proteins belonging to the Calvin cycle and glycolysis functional category we found the Rubisco large subunit, Rubisco activase, as well as Fructose bisphosphate aldolase 1 and 2. Previous experiments on *A. thaliana* have shown that light modulation of Rubisco large subunit is mainly due to activity regulation of Rubisco activase by redox changes [42, 43]. In addition, it has also been reported that Rubisco activity is modulated by cysteine-thiol groups oxidation [44], and by S-nitrosylation [45]. The redox regulation of these two proteins may act as an on/off switch to prevent the futile cycling of Calvin cycle intermediates in the dark, which wastes energy [46]. In this study we reported that TYR nitration, as key process of redox signaling, could be involved in Rubisco large subunit and Rubsico activase modulation during plant defence response. In particular, the nitrated Rubisco large subunit isoforms are detected only after 4 and 8 h of pathogen exposure. The functional significance of Rubisco nitration modulation during the HR remains unclear. Previous findings have shown that the phosphorylated isoform of Rubisco large subunit was significantly increased in the *A. thaliana* plants undergoing HR [47]. Here, we report the same modulation also for the nitrated isoform. Our findings are in line with the previous studies showing a dynamic interplay between nitration and phosphorylation in redox signaling [48, 49]. As

 

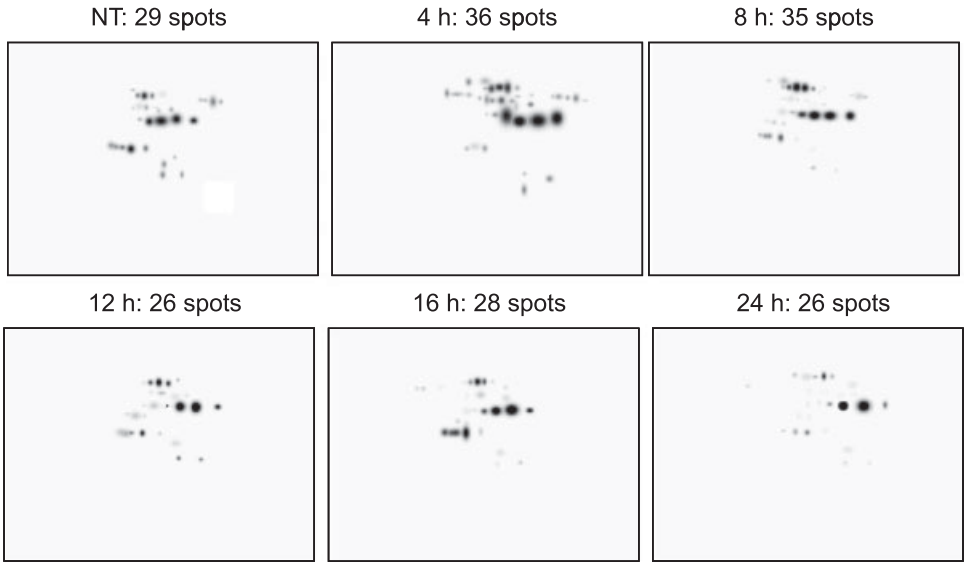


**Figure 4.** Image analysis of immunopositive protein spots. 2D-WB standard images of protein extract from *A. thaliana* control (NT), and 4, 8, 12, 16, and 24 h after infiltration with avirulent Pst together with the different immunopositive counted spots (29, 36, 35, 26, 28, and 26) are shown.

regarding Fructose bisphosphate aldolase 1 and 2 (FBA1 and FBA2) they are glycolytic and Calvin cycle enzymes, of chloroplast (FBA1) and cytosol (FBA2), catalyzing the reversible cleavage of fructose-1,6-bisphosphate into dihydroxyacetone-phosphate and glyceraldehyde 3-phosphate. FBA1 is the target of glutathionylation in *A. thaliana* during modulation of sugar metabolism in response to changing light conditions and environmental stresses [50]. It has been proposed that inactivation of FBA1 by glutathionylation slow down glycolysis and the tricarboxylic acid cycle, leading to mitochondrial metabolism and ROS production arrest. It is possible to speculate that nitration of FBA1 and FBA2, as reported in this study, could play an analog role in the regulation of enzyme activity. Up to now, such a redox regulation of FBA has been demonstrated only in mammalian cells under inflammatory-associated diseases [51]. On the other hand, FBA upregulation has been reported in ascorbate-deficient mutants of *A. thaliana* during oxidative stress [35]. Finally, among the nitrated proteins involved in nitrate assimilation we identified Glutamine synthetase 2 (GS2). GS2 plays an essential role in the metabolism of nitrogen by catalyzing the condensation of glutamate and ammonia to form glutamine [52]. Nitrogen nutrition has a significant impact on plant disease development: reduced availability of nitrogen often increases the susceptibility of plants to diseases [53]. It has been demonstrated that tomato leaves infected by different viruses, as well as exposed to oxidative stress, show reduced level of GS2 expression [54]. Moreover, it has been already reported that the tabtoxin produced by *P. syringae* inhibits the GS activity of the host plant, resulting in chlorosis of the leaves and senescence-like symptoms [55]. In this study we have shown the upregulation of nitrated GS2 in *A. thaliana* during the HR, suggesting that GS2 tyrosine nitration could be associated with inactivation.

In conclusion, this study represents the first contribution to identify the proteins that are target of nitration during the plant hypersensitive disease resistance response. Taken together, our results support the conclusion that defence response in *A. thaliana* is correlated with a modulation of nitrated proteins involved in important cellular process, such as photosynthesis, glycolysis and nitrate assimilation. The identification of nitrated proteins, whose expression and level of nitration are altered during the HR, may contribute to improve the understanding of defense response and the mechanisms mediating plant–pathogen interaction. Notwithstanding, further analysis will be required to understand the functional significance of nitration modulation. These findings might have applications in future, especially in the field of biotechnologies, for the improvement of plant defense response against pathogen attacks.

*L. Z. was financially supported by the Italian Ministry for University and Research (MIUR-PRIN 2006) and by the National Blood Centre (ISS). M. D. acknowledges support by the EMBO Young Investigators Program. This work was supported by a grant to M. D. from the Ministero dell'Università e della Ricerca in the framework of the program 'Components of the nitric oxide signalling pathways in plants'.*

*The authors have declared no conflict of interest.*

## 5 References

[1] Neill, S. J., Desikan, R., Clarke, A., Hurst, R. D., Hancock, J. T., *J. Exp. Bot.* 2002, *53*, 1237–1247.

[2] Lamattina, L., García-Mata, C., Graziano, M., Pagnussat, G., *Annu. Rev. Plant Biol.* 2003, *54*, 109–136.

[3] Neill, S., Barros, R., Bright, J., Desikan, R., Hancock, J., Harrison, J., Morris, P. *et al.*, *J. Exp. Bot.* 2008, *59*, 165–176.

 

[4] Delledonne, M., *Curr. Opin. Plant Biol.* 2005, *8*, 390–396.

[5] Lamb, C., Dixon, R. A., *Annu. Rev. Plant Physiol. Plant Mol. Biol.* 1997, *48*, 251–275.

[6] Greenberg, J. T., Yao, N., *Cell. Microbiol.* 2004, *6*, 201–211.

[7] Ryals, J. A., Neuenschwander, U. H., Willits, M. G., Molina, A., Steiner, H. Y., Hunt, M. D., *Plant Cell* 1996, *8*, 1809–1819.

[8] Keller, T., Damude, H. G., Werner, D., Doerner, P., Dixon, R. A., Lamb, C., *Plant Cell* 1998, *10*, 255–266.

[9] Delledonne, M., Xia, Y., Dixon, R. A., Lamb, C., *Nature* 1998, *394*, 585–588.

[10] Delledonne, M., Zeier, J., Marocco, A., Lamb, C., *Proc. Natl. Acad. Sci. USA* 2001, *98*, 13454–13459.

[11] Zago, E., Morsa, S., Dat, J. F., Alard, P., Ferrarini, A., Inzé, D., Delledonne, M., Van Breusegem, F., *Plant Physiol.* 2006, *141*, 404–411.

[12] Koppenol, W. H., Moreno, J. J., Pryor, W. A., Ischiropoulos, H., Beckman, J. S., *Chem. Res. Toxicol.* 1992, *5*, 834–842.

[13] Beckman, J. S., Koppenol, W. H., *Am. J. Physiol.* 1996, *271*, C1424–C1437.

[14] Romero-Puertas, M. C., Perazzolli, M., Zago, E. D., Delledonne, M., *Cell. Microbiol.* 2004, *6*, 795–803.

[15] Radi, R., *Proc. Natl. Acad. Sci. USA* 2004, *101*, 4003–4008.

[16] Kong, S. K., Yim, M. B., Stadtman, E. R., Chock, P. B., *Proc. Natl. Acad. Sci. USA* 1996, *93*, 3377–3382.

[17] Monteiro, H. P., *Free Radic. Biol. Med.* 2002, *33*, 765–773.

[18] Brito, C., Naviliat, M., Tiscornia, A. C., Vuillier, F., Gualco, G., Dighiero, G., Radi, R., Cayota, A. M., *J. Immunol.* 1999, *162*, 3356–3366.

[19] Morot-Gaudry-Talarmain, Y., Rockel, P., Moureaux, T., Quilleré, I., Leydecker, M. T., Kaiser, W. M., Morot-Gaudry, J. F., *Planta* 2002, *215*, 708–715.

[20] Saito, S., Yamamoto-Katou, A., Yoshioka, H., Doke, N., Kawakita, K., *Plant Cell Physiol.* 2006, *47*, 689–697.

[21] Valderrama, R., Corpas, F. J., Carreras, A., Fernández-Ocaña, A., Chaki, M., Luque, F., Gómez-Rodríguez, M. V. *et al*., *FEBS Lett.* 2007, *581*, 453–461.

[22] Corpas, F. J., Chaki, M., Fernández-Ocaña, A., Valderrama, R., Palma, J. M., Carreras, A., Begara-Morales, J. C. *et al*., *Plant Cell Physiol.* 2008, *49*, 1711–1722.

[23] Romero-Puertas, M. C., Laxa, M., Mattè, A., Zaninotto, F., Finkemeier, I., Jones, A. M., Perazzolli, M. *et al*., *Plant Cell* 2007, *19*, 4120–4130.

[24] Kav, N. N., Srivastava, S., Yajima, W., Sharma, N., *Curr. Proteomics* 2007, *4*, 28–43.

[25] Romero-Puertas, M. C., Campostrini, N., Mattè, A., Righetti, P. G., Perazzolli, M., Zolla, L., Roepstorff, P., Delledonne, M., *Proteomics* 2008, *8*, 1459–1469.

[26] Pryor, W. A., Squadrito, G. L., *Am. J. Physiol.* 1995, *268*, L699–L722.

[27] Laemmli, U. K., *Nature* 1970, *227*, 680–685.

[28] Cecconi, D., Zamò, A., Parisi, A., Bianchi, E., Parolini, C., Timperio, A. M., Zolla, L., Chilosi, M., *J. Proteome Res.* 2008, *7*, 2670–2680.

[29] Al-Shahrour, F., Díaz-Uriarte, R., Dopazo, J., *Bioinformatics* 2004, *20*, 578–580.

[30] Chu, H. A., Nguyen, A. P., Debus, R. J., *Biochemistry* 1994, *33*, 6150–6157.

[31] Suorsa, M., Aro, E. M., *Photosynth. Res.* 2007, *93*, 89–100.

[32] Murakami, R., Ifuku, K., Takabayashi, A., Shikanai, T., Endo, T., Sato, F., *FEBS J.* 2005, *272*, 2165–2175.

[33] Lundin, B., Nurmi, M., Rojas-Stuetz, M., Aro, E. M., Adamska, I., Spetea, C., *Photosynth. Res.* 2008, *98*, 405–414.

[34] Lundin, B., Hansson, M., Schoefs, B., Vener, A. V., Spetea, C., *Plant J.* 2007, *49*, 528–539.

[35] Giacomelli, L., Rudella, A., van Wijk, K. J., *Plant Physiol.* 2006, *141*, 685–701.

[36] Yamauchi, Y., Furutera, A., Seki, K., Toyoda, Y., Tanaka, K., Sugimoto, Y., *Plant Physiol. Biochem.* 2008, *46*, 786–793.

[37] Zaninotto, F., La Camera, S., Polverari, A., Delledonne, M., *Plant Physiol.* 2006, *141*, 379–383.

[38] Jones, A. M., Thomas, V., Bennett, M. H., Mansfield, J., Grant, M., *Plant Physiol.* 2006, *142*, 1603–1620.

[39] Loll, B., Kern, J., Saenger, W., Zouni, A., Biesiadka, J., *Nature* 2005, *438*, 1040–1044.

[40] González-Pérez, S., Quijano, C., Romero, N., Melø, T. B., Radi, R., Arellano, J. B., *Arch. Biochem. Biophys.* 2008, *473*, 25–33.

[41] Lindermayr, C., Saalbach, G., Durner, J., *Plant Physiol.* 2005, *137*, 921–930

[42] Zhang, N., Kallis, R. P., Ewy, R. G., Portis, A. R., Jr. *Proc. Natl. Acad. Sci. USA* 2002, *99*, 3330–3334.

[43] Portis, A. R., Jr., Li, C., Wang, D., Salvucci, M. E., *J. Exp. Bot.* 2008, *59*, 1597–1604.

[44] Moreno, J., García-Murria, M. J., Marín-Navarro, J., *J. Exp. Bot.* 2008, *59*, 1605–1614.

[45] Abat, J. K., Mattoo, A. K., Deswal, R., *FEBS J.* 2008, *275*, 2862–2872.

[46] Fridlyand, L. E., Backhausen, J. E., Scheibe, R., *Photosynth. Res.* 1999, *61*, 227–239.

[47] Jones, A. M., Bennett, M. H., Mansfield, J. W., Grant, M., *Proteomics* 2006, *6*, 4155–4165.

[48] Monteiro, H. P., Arai, R. J., Travassos, L. R., *Antioxid. Redox Signal* 2008, *10*, 843–889.

[49] Monteiro, H. P., *Free Radic. Biol. Med.* 2002, *33*, 765–773.

[50] Ito, H., Iwabuchi, M., Ogawa, K., *Plant Cell Physiol.* 2003, *44*, 655–660.

[51] Koeck, T., Levison, B., Hazen, S. L., Crabb, J. W., Stuehr, D. J., Aulak, K. S., *Mol. Cell. Proteomics* 2004, *3*, 548–557.

[52] Lightfoot, D. A., *Nucleic Acids Res.* 1988, *16*, 4164.

[53] Solomon, P. S., Tan, K. C., Oliver, R. P., *Mol. Plant Pathol.* 2003, *4*, 203–210.

[54] Pageau, K., Reisdorf-Cren, M., Morot-Gaudry, J. F., Masclaux-Daubresse, C., *J. Exp. Bot.* 2006, *57*, 547–557.

[55] Turner, J. G., Debbage, J. M., *Physiol. Plant Pathol.* 1982, *20*, 223–233.

 